arXiv:2209.03505v1 [hep-ex] 7 Sep 2022

Background Monte Carlo Samples for a Future Hadron Collider

Robert Gardner[1], Simone Pagan Griso[2], Stefan Hoeche[3], Karol Krizka[1], Fabio Maltoni[4], Andrew Melo[5], Meenakshi Narain[6], Isabel Ojalvo[7], Pascal Paschos[1], Laura Reina[8], Michael Schmitt[9], Horst Severini[10], Giordon Stark[11], John Stupak III*[10], Thiago Tomei[12], Alessandro Tricoli[13], and David Yu[6]

[1]Enrico Fermi Institute, University of Chicago
[2]Lawrence Berkeley National Laboratory
[3]Fermi National Accelerator Laboratory
[4]Centre for Cosmology, Particle Physics and Phenomenology, Université Catholique de Louvain
[5]Department of Physics, Vanderbilt University
[6]Department of Physics, Brown University
[7]Department of Physics, Princeton University
[8]Department of Physics, Florida State University
[9]Department of Physics, Northwestern University
[10]Homer L. Dodge Department of Physics & Astronomy, University of Oklahoma
[11]Santa Cruz Institute for Particle Physics, University of California, Santa Cruz
[12]Department of Physics, Sao Paulo State University
[13]Brookhaven National Laboratory

Submitted to the Proceedings of the US Community Study on the Future of Particle Physics (Snowmass 2021)

Abstract

A description of Standard Model background Monte Carlo samples produced for studies related to future hadron colliders.

1 Introduction

The final missing piece of the Standard Model (SM), the Higgs boson, was discovered in 2012 by the ATLAS and CMS experiments at the Large Hadron Collider (LHC) [1, 2]. However,

*john.stupak@ou.edu

the SM leaves several important questions unanswered, whose explanation requires Beyond the SM (BSM) physics. Despite the remarkable success of the LHC physics program, no statistically significant evidence for BSM physics has been observed.

The discovery of BSM physics may be just around the corner at the LHC. Alternatively, the mass scale of BSM physics may be outside the reach of the LHC, requiring a future high-energy collider to uncover. A $\sqrt{s} = 100$ TeV pp collider has therefore been proposed to eventually supplant the LHC [3].

The cross sections for SM background processes such as $V(W^{\pm}/Z)$+jets and $t\bar{t}$ are very large at $\sqrt{s} = 100$ TeV. Accurately modeling the tails of kinematic distributions for these processes requires production of sophisticated Monte Carlo (MC) samples with large statistics. The production of such samples, following an approach similar to that adopted for Snowmass 2013 [4, 5, 6], is described here.

2 Monte Carlo Simulation

High-statistic V + jets and $t\bar{t}$ background Monte Carlo samples were produced for $\sqrt{s} = 13$ and 100 TeV pp colliders, using MadGraph5_aMC@NLO v3.3.1 [7], Pythia8 v8.306 [8], and Delphes v3.5.0 [9], with computing resources provided by the Open Science Grid [10]. MadGraph5_aMC@NLO was used to simulate pp hard scatter matrix elements. Parton shower and hadronization were performed with Pythia8. Delphes parameterized detector simulation was used to account for the detector response.

2.1 Hard Scatter

Hard scatter matrix elements were computed in the four-flavor scheme at leading-order (LO) accuracy in the strong coupling constant with MadGraph5_aMC@NLO. On-shell heavy resonances (V, t, H) were treated as stable particles. Radiated partons are allowed (with transverse momentum $p_{\mathrm{T}} \geq 20$ GeV and pseudorapidity $|\eta| < 5$), up to a total of four final state particles. The `NNPDF31_nnlo_as_0118` parton distribution function was used [11].

So-called "gridpacks" were produced for streamlined operation on the OSG computing grid using the `makeGridpacks.sh` script, contained within the `MCProd` package (git tag: `v1.2nobias`).* Configuration cards can be found in the `Cards` directory.

2.2 Parton Shower

On-shell heavy resonances were decayed using Pythia8, neglecting spin correlation effects. Parton shower and hadronization were also simulated with Pythia8, using the CMS `CP5` tune [12]. k_{T}-MLM matching and merging of radiation from the matrix-element and parton shower was performed using the MG5aMC_PY8_interface [13]. For the V + jets ($t\bar{t}$)

*https://github.com/Snowmass21-software/MCProd/releases/tag/v1.2nobias

samples, a matching scale XQCUT = 40 (80) GeV was used. In both cases, QCUT is taken to be 1.5 × XQCUT.

2.3 Detector Response

The detector response was simulated using DELPHES. The parameterized detector performance is based on test beam data and full-simulation of a future FCC-hh detector [14]. The effect of pileup interactions is not simulated explicitly; instead, the parameterized efficiency and resolution for various physics objects include the expected degradation due to pileup interactions.

2.4 Workflow

A summary of the production workflow is shown in Fig. 1. The MADGRAPH5_AMC@NLO output (a standard LHE file [15]) serves as input to PYTHIA8. The PYTHIA8 output (in HepMC format [16]) serves as input to both RIVET and DELPHES. DELPHES produces a standard ROOT output [17], while RIVET produces output in the YODA format [18]. In addition to storing the final outputs from this workflow, intermediate outputs are retained as well.

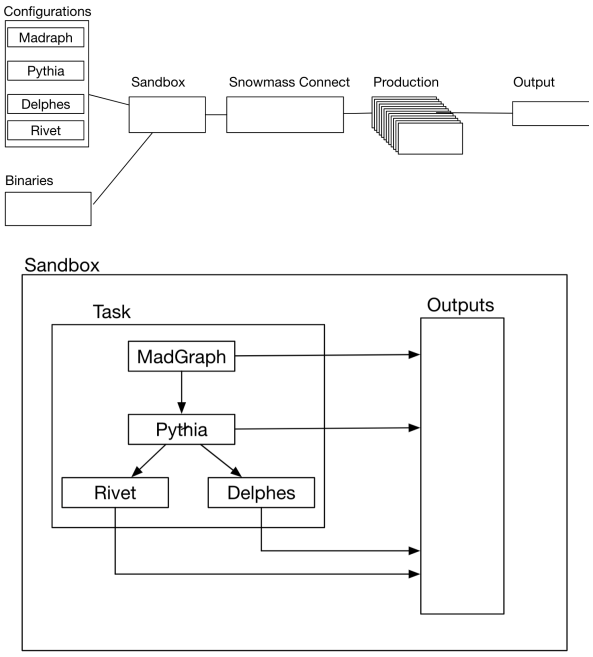


Figure 1: A summary of the production workflow.

3 Validation

Validation of the matching/merging of phase space for parton emission covered by the matrix element and parton shower is performed by studying differential jet rates. Comparison of the $\sqrt{s} = 13$ TeV samples to unfolded LHC data was performed using RIVET [18].

3.1 Matching/Merging

Suitability of the matching/merging settings is confirmed based on the differential jet rates, shown for $\sqrt{s} = 100$ TeV W + jets events in Figure 2. Similar plots for Z + jets and $t\bar{t}$ samples are shown in the appendix. These observables represent the scale at which an N-jet event transitions to an $N + 1$-jet event, and exhibit a smooth transition.

3.2 Comparison to Data

The RIVET toolkit provides a convenient mechanism to compare simulated MC to unfolded collider data, using a variety of predefined analysis routines.

The W + jets sample was validated using the `CMS_2017_I1610623` routine, which targets $W(\to \mu\nu)$+jets production. This routine selects events with a muon and transverse mass $m_{\mathrm{T}} \geq 50$ GeV. Muons are required to have $p_{\mathrm{T}} \geq 25$ GeV and $|\eta| < 2.4$.

The Z + jets sample was validated using the `CMS_2019_I1753680` routine, which targets $Z(\to \ell\ell)$+jets production, where $\ell = e/\mu$. This routine selects events with a pair of opposite-sign electrons or muons. In both cases, electrons and muons are required to have $p_{\mathrm{T}} \geq 25$ GeV and $|\eta| < 2.4$.

The $t\bar{t}$ sample was validated using the `CMS_2018_I1663958` routine, which targets events with semi-leptonic decay of top pairs. This routine selects events with an electron or muon (with $p_{\mathrm{T}} \geq 30$ GeV and $|\eta| < 2.4$). W and t candidates are formed from the lepton, jets and missing transverse energy $\not{E}_T$, by minimizing the difference between the true mass and the reconstructed mass for these candidates.

4 Results

Cross sections for $\sqrt{s} = 13$ and 100 TeV background processes are given in Table 1.

	W + jets	Z + jets	$t\bar{t}$
$\sigma_{13\ \mathrm{TeV}}$ [nb]	184.7	56.05	0.6137
$\sigma_{100\ \mathrm{TeV}}$ [nb]	1,428	471.1	36.47

Table 1: Calculated cross sections for SM background processes at $\sqrt{s} = 13$ and 100 TeV.

A comparison of the $\sqrt{s} = 13$ TeV simulation and data is shown in Figures 3, 4, and

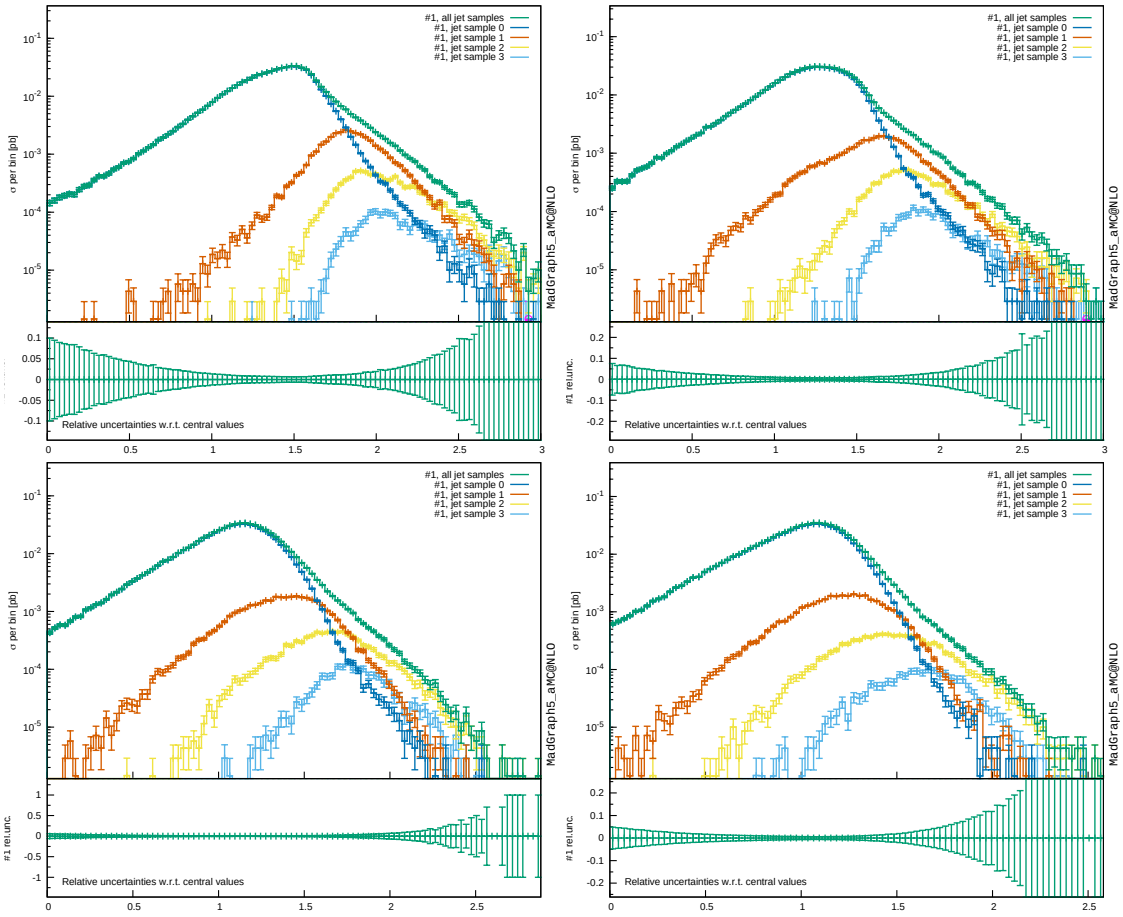


Figure 2: Differential jet rate distributions for $\sqrt{s} = 100$ TeV $W+$jets events, showing $\log_{10}$ of the merging scale. The upper left (right) plot represents a transition from a 0-jet event to a 1-jet (1-jet event to a 2-jet) event. The lower left (right) plot represents a transition from a 2-jet event to a 3-jet (3-jet event to a 4-jet) event.

5, for W + jets, Z + jets, and $t\bar{t}$ samples, respectively. Additional comparison plots are available on the web.[†] The agreement between simulated Z + jets and $t\bar{t}$ samples and data is reasonable; while the overall discrepancy is approximately 10%, the shapes are not generally well reproduced in the simulation, leading to bin-by-bin discrepancies of up to 50% or more in certain regions of phase space. The agreement between the simulated W + jets and data is worse, at the 50%-level overall. There is a general overproduction of jets, particularly at high p_T. The source of this discrepancy is under investigation. However, some event shapes are well described by the simulation.

5 Conclusion

The production of SM background MC samples for $\sqrt{s} = 13$ and 100 TeV pp colliders has been described. A comparison of the $\sqrt{s} = 13$ TeV simulation to data from the LHC was performed. While the agreement between simulated Z + jets and $t\bar{t}$ events and collision data is reasonable, the modeling of W + jets events is not acceptable. The source of this mismodeling is under investigation. Due to the similarities in production between the W + jets and Z + jets/$t\bar{t}$ samples, we do not advise using any of these samples for physics studies, until the discrepancy is understood.

ACKNOWLEDGEMENTS

This research was done using services provided by the OSG Consortium [10, 19], which is supported by the National Science Foundation awards #2030508 and #1836650. We would also like to thank Olivier Mattelaer for significant MadGraph5_aMC@NLO assistance.

References

[1] S. Chatrchyan, V. Khachatryan, A. Sirunyan, A. Tumasyan, W. Adam, E. Aguilo et al., *Observation of a new boson at a mass of 125 GeV with the CMS experiment at the LHC*, *Physics Letters B* **716** (2012) 30 [1207.7235].

[2] G. Aad, T. Abajyan, B. Abbott, J. Abdallah, S. Abdel Khalek, A. Abdelalim et al., *Observation of a new particle in the search for the Standard Model Higgs boson with the ATLAS detector at the LHC*, *Physics Letters B* **716** (2012) 1 [1207.7214].

[3] FCC collaboration, *FCC-hh: The Hadron Collider: Future Circular Collider Conceptual Design Report Volume 3*, *European Physical Journal Special Topics* **228** (2019) 755.

[†] W + jets: https://jstupak.web.cern.ch/noBias/W/,
Z + jets: https://jstupak.web.cern.ch/noBias/Z/,
$t\bar{t}$: https://jstupak.web.cern.ch/noBias/tt/

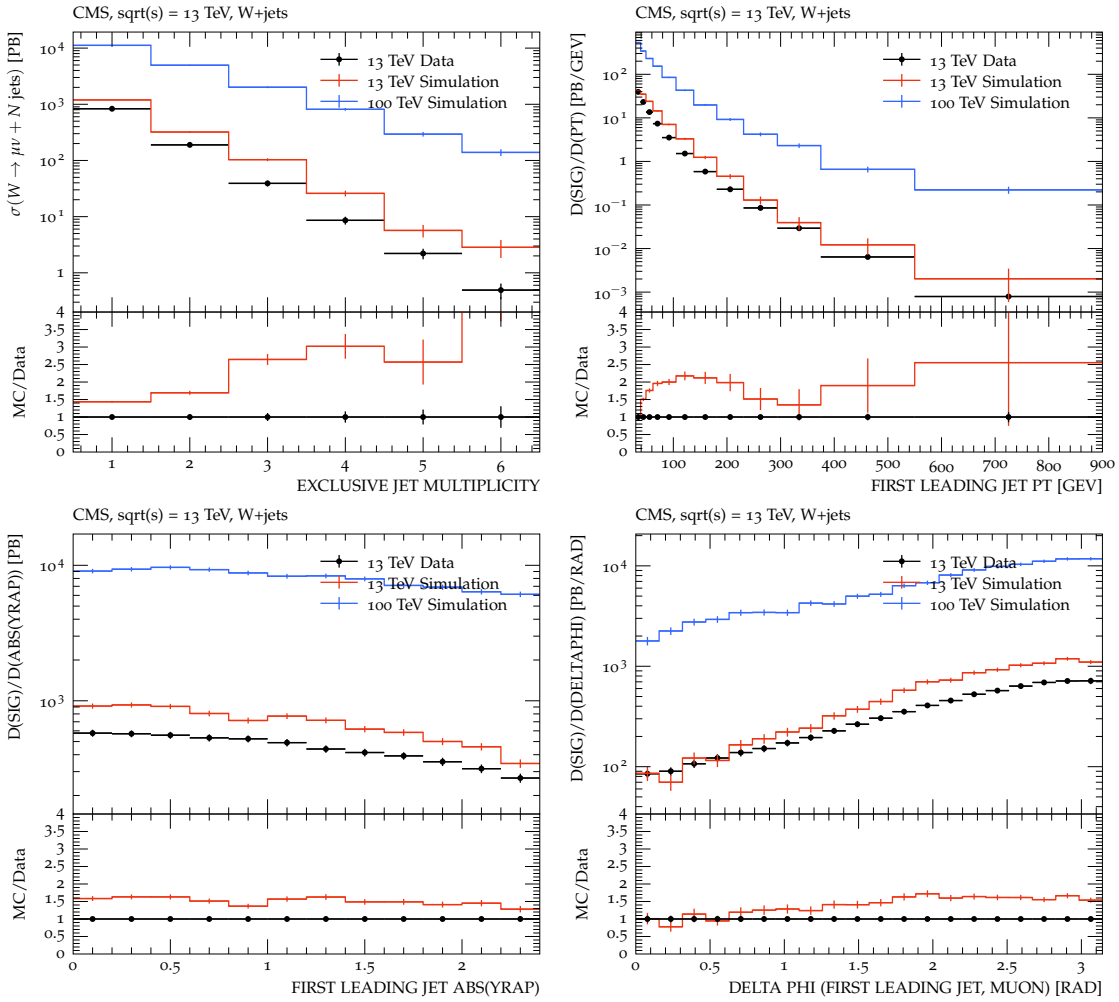


Figure 3: A comparison of $\sqrt{s} = 13$ TeV $W+$jets data and simulation, as well as results for $\sqrt{s} = 100$ TeV simulation. The upper left (right) plot shows the exclusive jet multiplicity (leading jet p_T). The lower left (right) plot shows the leading jet rapidity y (difference in azimuthal angle between the selected muon and leading jet).

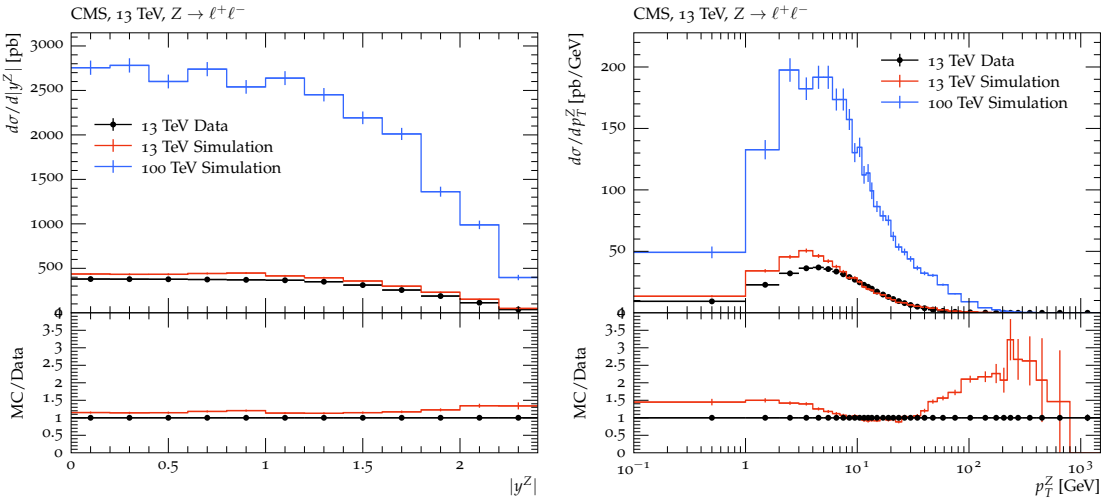


Figure 4: A comparison of $\sqrt{s} = 13$ TeV $Z+$jets data and simulation, as well as results for $\sqrt{s} = 100$ TeV simulation. The left (right) plot shows the Z boson y (p_T).

[4] A. Avetisyan, S. Bhattacharya, M. Narain, S. Padhi, J. Hirschauer, T. Levshina et al., *Snowmass Energy Frontier Simulations using the Open Science Grid (A Snowmass 2013 whitepaper)*, 1308.0843.

[5] J. Anderson, A. Avetisyan, R. Brock, S. Chekanov, T. Cohen, N. Dhingra et al., *Snowmass Energy Frontier Simulations*, 1309.1057.

[6] A. Avetisyan, J.M. Campbell, T. Cohen, N. Dhingra, J. Hirschauer, K. Howe et al., *Methods and Results for Standard Model Event Generation at $\sqrt{s}$ = 14 TeV, 33 TeV and 100 TeV Proton Colliders (A Snowmass Whitepaper)*, 1308.1636.

[7] J. Alwall, R. Frederix, S. Frixione, V. Hirschi, F. Maltoni, O. Mattelaer et al., *The automated computation of tree-level and next-to-leading order differential cross sections, and their matching to parton shower simulations*, *Journal of High Energy Physics* **2014** (2014) 79 [1405.0301].

[8] C. Bierlich, S. Chakraborty, N. Desai, L. Gellersen, I. Helenius, P. Ilten et al., *A comprehensive guide to the physics and usage of PYTHIA 8.3*, 2203.11601.

[9] J. de Favereau, C. Delaere, P. Demin, A. Giammanco, V. Lemaître, A. Mertens et al., *DELPHES 3: a modular framework for fast simulation of a generic collider experiment*, *Journal of High Energy Physics* **2014** (2014) 57 [1307.6346].

[10] R. Pordes, D. Petravick, B. Kramer, D. Olson, M. Livny, A. Roy et al., *The open science grid*, *Journal of Physics: Conference Series* **78** (2007) 012057.

[11] R.D. Ball, V. Bertone, S. Carrazza, L.D. Debbio, S. Forte, P. Groth-Merrild et al., *Parton distributions from high-precision collider data*, *European Physical Journal C* **77** (2017) 663 [1706.00428].

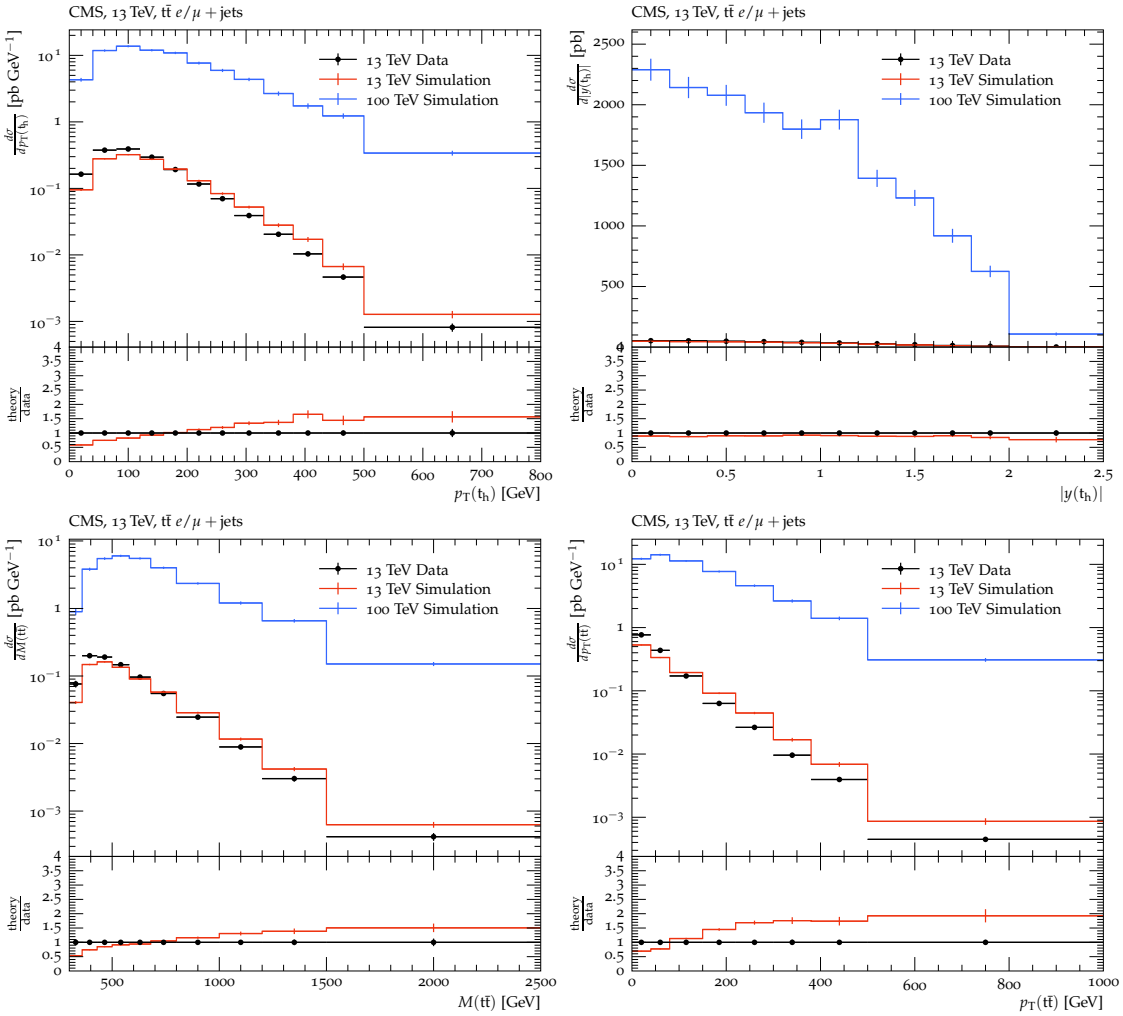


Figure 5: A comparison of $\sqrt{s} = 13$ TeV $t\bar{t}$ data and simulation, as well as results for $\sqrt{s} = 100$ TeV simulation. The upper left (right) plot shows the hadronic top p_T (y). The lower left (right) plot shows the invariant mass m (p_T) of the top-pair system.

[12] V. Khachatryan, A.M. Sirunyan, A. Tumasyan, W. Adam, E. Asilar, T. Bergauer et al., *Event generator tunes obtained from underlying event and multiparton scattering measurements*, *European Physical Journal C* **76** (2016) 155 [1512.00815].

[13] J. Alwall et al., *Comparative study of various algorithms for the merging of parton showers and matrix elements in hadronic collisions*, *European Physical Journal C* **53** (2008) 473 [0706.2569].

[14] M. Selvaggi, "A Delphes parameterisation of the FCC-hh detector." https://cds.cern.ch/record/2717698, 2020.

[15] J. Alwall et al., *A Standard format for Les Houches event files*, *Computer Physics Communications* **176** (2007) 300 [0609017].

[16] A. Buckley, P. Ilten, D. Konstantinov, L. Lönnblad, J. Monk, W. Pokorski et al., *The HepMC3 event record library for Monte Carlo event generators*, *Computer Physics Communications* **260** (2021) 107310 [1912.08005].

[17] R. Brun, F. Rademakers, P. Canal, A. Naumann, O. Couet, L. Moneta et al., *root-project/root: v6.18/02*, 2019. 10.5281/zenodo.3895860.

[18] C. Bierlich, A. Buckley, J. Butterworth, C.H. Christensen, L. Corpe, D. Grellscheid et al., *Robust Independent Validation of Experiment and Theory: Rivet version 3*, *SciPost Physics* **8** (2020) 026 [1912.05451].

[19] I. Sfiligoi, D.C. Bradley, B. Holzman, P. Mhashilkar, S. Padhi and F. Wurthwrin, *The pilot way to Grid resources using glideinWMS*, *WRI World Congress* **2** (2009) 428.

A Supplementary Results

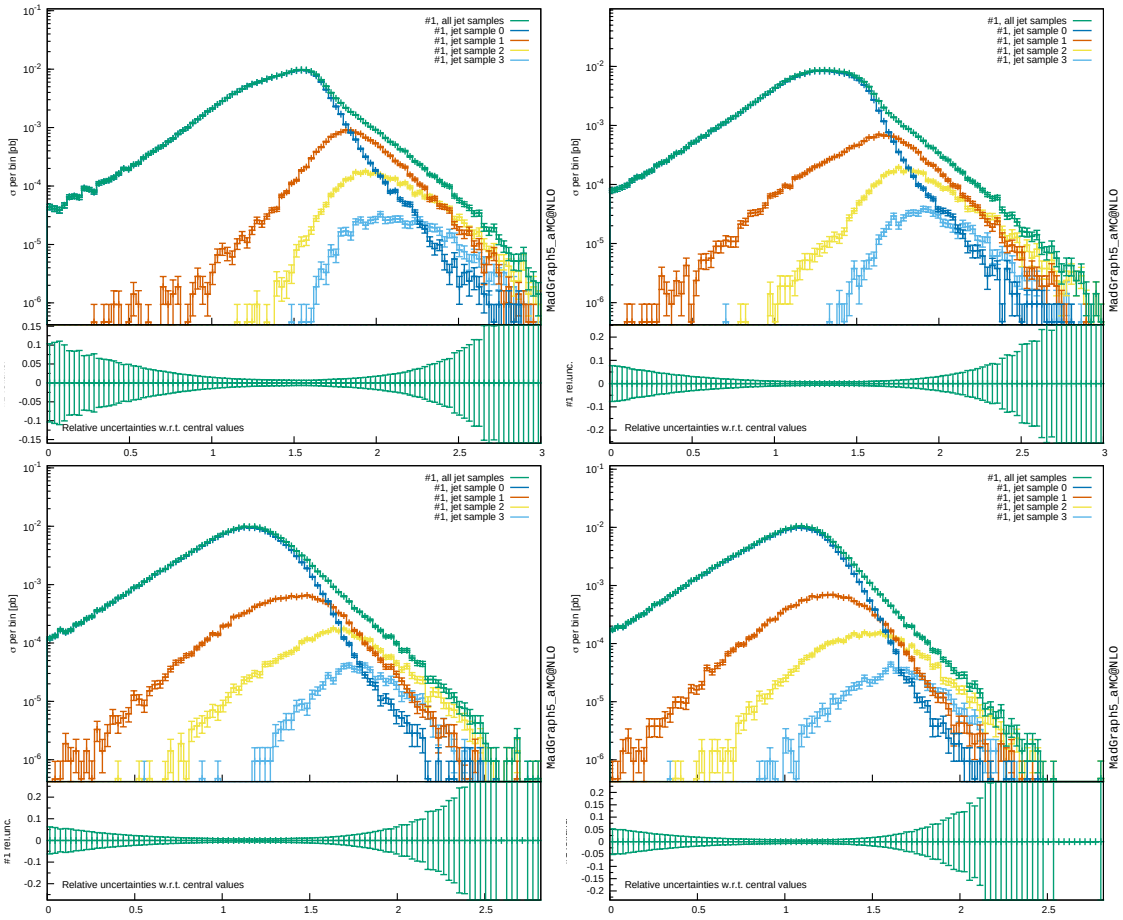


Figure 6: Differential jet rate distributions for $\sqrt{s} = 100$ TeV $Z+$jets events, showing $\log_{10}$ of the merging scale. The upper left (right) plot represents a transition from a 0-jet event to a 1-jet (1-jet event to a 2-jet) event. The lower left (right) plot represents a transition from a 2-jet event to a 3-jet (3-jet event to a 4-jet) event.

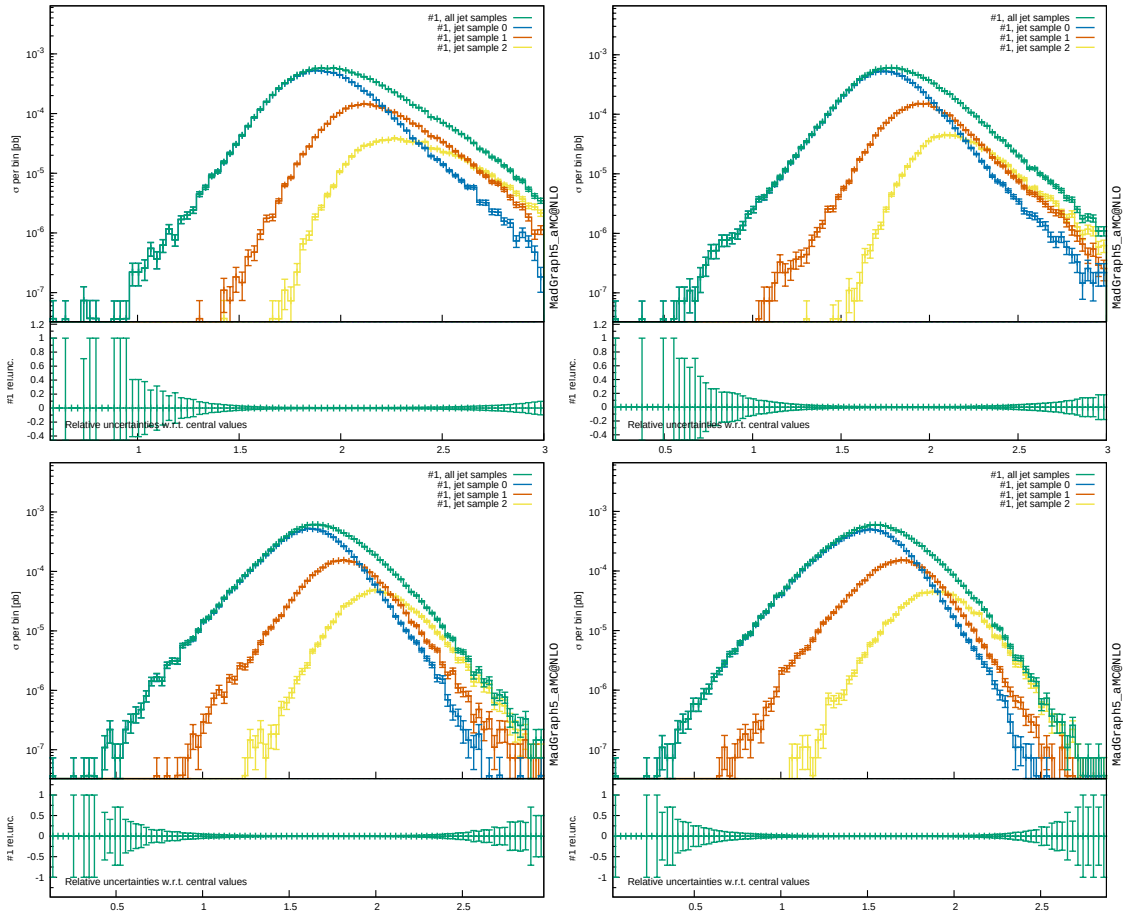


Figure 7: Differential jet rate distributions for $\sqrt{s} = 100$ TeV $t\bar{t}$ events, showing $\log_{10}$ of the merging scale. The upper left (right) plot represents a transition from a 0-jet event to a 1-jet (1-jet event to a 2-jet) event. The lower left (right) plot represents a transition from a 2-jet event to a 3-jet (3-jet event to a 4-jet) event.